Proceedings of the 28th IEEE
EMBS Annual International Conference
New York City, USA, Aug 30-Sept 3, 2006

Ordinary differential equation models for ethanol pharmacokinetic based on anatomy and physiology

Jae-Joon Han, Martin H. Plawecki, Peter C. Doerschuk, Vijay A. Ramchandani, and Sean O'Connor

Abstract— **Physiologically-based pharmacokinetic (PBPK) models have been used to describe the distribution and elimination characteristics of intravenous ethanol administration. Further, these models have been used to estimate the ethanol infusion profile required to prescribe a specific breath ethanol concentration time course in a specific human being, providing a platform upon which other pharmacokinetic and pharmacodynamic investigations are based. In these PBPK models, the equivalence of two different peripheral tissue models are shown and issues concerning the mass flow into the liver in comparison with ethanol metabolism in the liver are explained.**

I. Introduction

Nearly eight percent of people who use ethanol, will become addicted during the course of their life, and about a third of them will die of complications attributable to ethanol [1], [2]. A major factor underlying the brain's exposure to ethanol[1] is its pharmacokinetics, that is, the relationship between ethanol intake through various paths (e.g., oral, intravenous) and its resulting concentration in various tissues over time [3].

Administering ethanol and measuring the resulting tissue concentrations of ethanol is a challenging problem in human subjects, and controlling those concentrations is even more difficult. First, the pharmacodynamic effects of ethanol occur in the brain, but it cannot be directly administered to the brain. Second, given the same administration, even by infusion, the time course of flow and accumulation of ethanol varies considerably in subjects whose size and body composition differ. Finally, it is currently impossible to measure brain ethanol concentration in humans directly.

Certain assumptions and methods make intermittent approximate measurement of brain ethanol concentration possible. It is reasonable to assume that brain and arterial blood ethanol concentrations are equal, due to the high brain blood flow rate relative to its small water volume. Further, use of a breath test on end-expiratory air gives a good approximation to arterial ethanol concentration. However, the breath test can only be effectively used in a laboratory or a forensic environment and the continuous measurement of the breath alcohol concentration is not yet possible. Therefore, mathematical models relating various input dose and various concentration trajectories are critical to studying ethanol. This paper studies and further develops one prominent model, the so-called physiologically-based pharmacokinetic model (PBPK model) [4]–[11], developed at the Indiana Alcohol Research Center of the Indiana University School of Medicine. The PBPK model maintains a balance between physiologic fidelity (the number of pathways and parameters) and research utility (reliable prediction of brain exposure for an individual) by making every parameter physiologic, but minimizing their number.

The first contribution of this paper is to describe the PBPK model as a differential equation with a nonlinear constraint and then solve the constraint resulting in an unconstrained differential equation. The second contribution is to provide a graphical method for describing the PBPK model and related models that is analogous to a circuit diagram except that there are two "charges" flowing in the circuit, blood and ethanol. The third contribution is to show the equivalence among some different peripheral tissue models. The fourth contribution is to demonstrate that the standard PBPK model has anomalous behavior at low ethanol concentrations: the mass flow of ethanol being degraded can be greater than the total mass flow.

II. PBPK Model

We consider models that are interconnections of so-called "well stirred" compartments; when ethanol enters a compartment we assume that it is instantly spread uniformly throughout the compartment and so there is a single ethanol concentration for each compartment. The most complicated model we consider has three compartments which approximate the vasculature, liver, and all other tissues which we denote by periphery. Each compartment is described by giving the mass of ethanol in the compartment and the mathematical model for a compartment is a first-order nonlinear differential equation which describes the time rate of change of the mass of ethanol in the compartment. The interconnections between compartments transport ethanol and blood. The interconnections mimic vascular anatomy and physiology and include structures such as the portal vein and hepatic vein. The flux of ethanol into and out of a compartment depends on ethanol concentration differences.

This work was supported by NIH N01AA23102, P60 AA07611-16-17, and NIAA R01 AA12555-05.

M. H. Plawecki is with the Weldon School of Biomedical Engineering, Purdue University and the Indiana University School of Medicine. J.-J. Han and P. C. Doerschuk are with the School of Electrical and Computer Engineering, Purdue University. V. A. Ramchandani is with the National Institute on Alcohol Abuse and Alcoholism and previously with the Department of Medicine, Indiana University School of Medicine. S. O'Connor is with the Department of Psychiatry, Indiana University School of Medicine and the R. L. Roudebush VA Medical Center.

Corresponding author: P. C. Doerschuk, School of Electrical and Computer Engineering, Purdue University, 465 Northwestern Avenue, West Lafayette, IN 47907-2035, doerschu@ecn.purdue.edu, +1 765 494-1742.

[1]The pharmacokinetics of ethanol concerns the time course of ethanol biochemistry while the pharmacodynamics concerns the time course of ethanol's cognitive effects.

The vasculature compartment circulates ethanol through the system at physiologically relevant concentrations until elimination has been completed. The periphery compartment acts as a storage reservoir from which ethanol may enter or leave, based upon the gradients between its concentration and the arterial and venous ethanol concentrations respectively.

Ethanol enters the system through two pathways. The simpler pathway is by venous infusion, which occurs only in a laboratory setting. In this case the mass flow rate of ethanol is added directly to the well-stirred vascular compartment. The more complicated pathway is by oral intake. In this case the ethanol is transported through the proximal gut and is absorbed in the small intestine from which it enters the portal vein.

PBPK model elimination of ethanol occurs only in the liver compartment, and emulates a single enzyme system which follows Michaelis-Menten (MM) kinetics. In fact, three enzyme systems make up the major ethanol elimination pathways within the liver. However, *in vivo* determination of their individual characteristics is impossible and for that reason they are lumped into one pathway in this model. In addition, elimination from the other compartments is considered negligible, which is supported by animal studies [12].

An important part of the model is the transport of ethanol. The generic description of ethanol transport is

$$M_{x,y}(t) \quad = \quad k_{x,y} R_x r(C_y(t) - C_x(t)) \tag{1}$$

where $M_{x,y}(t)$ [Mass]/[Time] is the mass flux of ethanol from x to y at time t; $C_x(t)$ and $C_y(t)$ [Mass]/[Volume] are the concentrations of ethanol in x and y, respectively; $0 \leq k_{x,y} \leq 1$ is a dimensionless constant; R_x [Volume]/[Time] is the volume flow of blood in x, $r(\cdot)$ is the unit ramp defined by $r(x) = xu(x)$ where $u(\cdot)$ is the unit step function. The $r(\cdot)$ is used so that $M_{x,y}(t)$ does not have a negative value, which is not physiological.

The models described in this paper are roughly similar to electrical circuits and a graphical description similar to a circuit diagram is useful in understanding what is and what is not included in the model. Such a circuit diagram for a three-compartment model is shown in Fig. 1(a) where the block diagram fragments labeled A' and B' are to be ignored.

Each compartment in the block diagram of Fig. 1(a) is labeled with its name, its volume ($V_{\mathcal{X}}$ variable) and its state variable [$\mu_{\mathcal{X}}(t)$ variable] which is the mass of ethanol in the compartment. In addition, $C_{\mathcal{X}}(t) \doteq \mu_{\mathcal{X}}(t)/V_{\mathcal{X}}(t)$ is the concentration of ethanol in the compartment. The compartment subscripts are $\mathcal{V}$ for the Vascular, $\mathcal{T}$ for the peripheral Tissue, and $\mathcal{L}$ for the Liver parenchyma.

Each edge of the graph is labeled with a name, if it clearly corresponds to a particular anatomical structure, and is labeled with the ethanol mass flow [$M_{\mathrm{X}}(t)$ variable] and the volume flow [$R_{\mathrm{X}}(t)$ variable] that occur along that edge. The edges are directed, which indicates the positive flux direction. In addition, $C_{\mathrm{X}}(t) \doteq M_{\mathrm{X}}(t)/R_{\mathrm{X}}(t)$ is the concentration of ethanol in the edge. The edge subscripts are A for Aorta, P for Peripheral artery, VC for Vena Cava, PV for Portal Vein, HA for Hepatic Artery, HV for Hepatic Vein, and Cap for peripheral Capillary bed.

The mass flows $M_{\mathrm{Gut}}(t)$ and $M_{\mathrm{Infuse}}(t)$ are the external inputs to the system and represent the flow of ethanol from the gut and from a venous infusion, respectively. The mass flow $M_{\mathrm{Metab}}(t)$ is the ethanol sink created by liver metabolism of ethanol.

There are three kinds of vertices in the graph. The first type is the compartment, where the entering and exiting edges form the right hand side of a differential equation for the state variable. The second type are vertices where only one edge enters (no symbol) which obey Kirchhoff's Current Law (KCL) and divide the input fluxes (ethanol mass and volume) among the edges that exit. The F_{X} constants indicate the fractional of the input that exits on each of the exiting edges. The subscripts are L for fraction of the cardiac output directed to the liver and PV for the fraction of the liver-directed cardiac output that is directed through the gut and the portal vein. The third type are vertices where only one edge exits (Σ symbol) which obey KCL and sum the input fluxes (ethanol mass and volume) in order to determine the fluxes (ethanol mass and volume) on the edge that exits. Since the second and third type of vertices both obey KCL they are really the same.

A. The 3-state model

The basic three-state model is the model shown in Fig. 1(a) and is a generalization of the standard PBPK model. The state equations can be read directly from Fig. 1(a):

$$\mathrm{d}\mu_{\mathcal{L}}/\mathrm{d}t(t) = M_{\mathrm{HA},\mathcal{L}}(t) + M_{\mathrm{PV},\mathcal{L}}(t) - M_{\mathcal{L},\mathrm{HV}}(t) - M_{\mathrm{Metab}}(t) \tag{2}$$

$$\mathrm{d}\mu_{\mathcal{T}}/\mathrm{d}t(t) = M_{\mathrm{P},\mathcal{T}}(t) - M_{\mathcal{T},\mathrm{P}}(t) \tag{3}$$

$$\mathrm{d}\mu_{\mathcal{V}}/\mathrm{d}t(t) = M_{\mathrm{Infuse}}(t) + M_{\mathrm{Gut}}(t) - M_{\mathrm{PV},\mathcal{L}}(t) + M_{\mathcal{T},\mathrm{P}}(t) - M_{\mathrm{P},\mathcal{T}}(t) - M_{\mathrm{HA},\mathcal{L}}(t) + M_{\mathcal{L},\mathrm{HV}}(t) \tag{4}$$

Equations for the six unknown mass fluxes can be derived in terms of the three state variables. The mass flux from the liver parenchyma out of the system, which is denoted by $M_{\mathrm{Metab}}(t)$, is directly determined by MM kinetics:

$$M_{\mathrm{Metab}}(t) = V_{\max}\mu_{\mathcal{L}}(t)/(K_m + \mu_{\mathcal{L}}(t)/V_{\mathcal{L}}). \tag{5}$$

The remaining five unknown mass fluxes can be derived following the general principle that results in (1).

$$M_{\mathrm{P},\mathcal{T}}(t) = k_{\mathrm{P},\mathcal{T}} R_{\mathrm{A}}(1 - F_{\mathrm{L}}) r\left(\mu_{\mathcal{V}}(t)/V_{\mathcal{V}} - \mu_{\mathcal{T}}(t)/V_{\mathcal{T}}\right) \tag{6}$$

$$M_{\mathcal{T},\mathrm{P}}(t) = k_{\mathcal{T},\mathrm{P}} R_{\mathrm{A}}(1 - F_{\mathrm{L}}) r\left(\mu_{\mathcal{T}}(t)/V_{\mathcal{T}} - \mu_{\mathcal{V}}(t)/V_{\mathcal{V}}\right) \tag{7}$$

$$M_{\mathrm{HA},\mathcal{L}}(t) = k_{\mathrm{HA},\mathcal{L}} R_{\mathrm{A}} F_{\mathrm{L}}(1 - F_{\mathrm{PV}}) r(\mu_{\mathcal{V}}(t)/V_{\mathcal{V}} - \mu_{\mathcal{L}}(t)/V_{\mathcal{L}}) \tag{8}$$

$$M_{\mathrm{PV},\mathcal{L}}(t) = k_{\mathrm{PV},\mathcal{L}} R_{\mathrm{A}} F_{\mathrm{L}} F_{\mathrm{PV}} r(\mu_{\mathcal{V}}(t)/V_{\mathcal{V}} + M_{\mathrm{Gut}}(t)/R_{\mathrm{A}} F_{\mathrm{L}} F_{\mathrm{PV}} - \mu_{\mathcal{L}}(t)/V_{\mathcal{L}}) \tag{9}$$

$$M_{\mathcal{L},\mathrm{HV}}(t) = k_{\mathcal{L},\mathrm{HV}} R_{\mathrm{A}} F_{\mathrm{L}} r\left(\mu_{\mathcal{L}}(t)/V_{\mathcal{L}} - C_{\mathrm{HV}}(t)\right); \tag{10}$$

$M^{(2)}_{\mathrm{PV}}(t)$ and $M_{\mathrm{HA}}(t)$ ((11) and (12)),

$$M^{(2)}_{\mathrm{PV}}(t) \quad = \quad \mu_{\mathcal{V}}(t)/V_{\mathcal{V}} R_{\mathrm{A}} F_{\mathrm{L}} F_{\mathrm{PV}} + M_{\mathrm{Gut}}(t) \tag{11}$$

$$M_{\mathrm{HA}}(t) \quad = \quad R_{\mathrm{A}} F_{\mathrm{L}}(1 - F_{\mathrm{PV}}) \mu_{\mathcal{V}}(t)/V_{\mathcal{V}} \tag{12}$$

needed to evaluate

$\alpha(t)=(M_{\rm HA}(t)-M_{{\rm HA},\mathcal{L}}(t)+M^{(2)}_{\rm PV}(t)-M_{{\rm PV},\mathcal{L}}(t))/(R_{\rm A}F_{\rm L})$;

$\gamma(t) = \mu_{\mathcal{L}}(t)/V_{\mathcal{L}}$; and $C_{\rm HV}(t) = (\alpha(t)+k_{\mathcal{L},{\rm HV}}\gamma(t))/(1+k_{\mathcal{L},{\rm HV}})$ for $\alpha(t) < \gamma(t)$ and $C_{\rm HV}(t)=\alpha(t)$ for $\alpha(t)>\gamma(t)$. The following constants are required: the volumes of the three compartments, denoted by $V_{\mathcal{V}}$, $V_{\mathcal{L}}$, and $V_{\mathcal{T}}$; the MM constants, denoted by $V_{\max}$ and K_m; the cardiac output, denoted by $R_{\rm A}$; the fraction of cardiac output that is delivered to the liver and the fraction of the total liver supply that is delivered by the portal vein, denoted by $F_{\rm L}$ and $F_{\rm PV}$, respectively, and the fraction of ethanol in a vessel or compartment that is transported to a connected vessel or compartment, denoted by $k_{{\rm P},\mathcal{T}}$, $k_{\mathcal{T},{\rm P}}$, $k_{{\rm HA},\mathcal{L}}$, $k_{{\rm PV},\mathcal{L}}$, and $k_{\mathcal{L},{\rm HV}}$.

B. The 2-state model

If we consider a second model which is the block diagram shown in Fig. 1(a) with A replaced by A', it has only two states and does not require a value for $V_{\mathcal{L}}$. This model is the standard PBPK model. The resulting equations are

$$\mathrm{d}\mu_{\mathcal{T}}/\mathrm{d}t(t) = M_{{\rm P},\mathcal{T}}(t) - M_{\mathcal{T},{\rm P}}(t) \quad (13)$$

$$\begin{aligned}\mathrm{d}\mu_{\mathcal{V}}/\mathrm{d}t(t) = &-R_{\rm A}F_{\rm L}\mu_{\mathcal{V}}(t)/V_{\mathcal{V}} + M_{\mathcal{T},{\rm P}}(t) - M_{{\rm P},\mathcal{T}}(t)\\ &+ r[R_{\rm A}F_{\rm L}\mu_{\mathcal{V}}(t)/V_{\mathcal{V}} + M_{\rm Gut}(t)\\ &- M_{\rm Metab}(t)] + M_{\rm Infuse}(t)\end{aligned} \quad (14)$$

$$M_{\rm Metab}(t) = M_{\max}C_{\mathcal{L}}(t)/(K_m + C_{\mathcal{L}}(t)) \quad (15)$$

$$C_{\mathcal{L}}(t) = \mu_{\mathcal{V}}(t)/V_{\mathcal{V}} + M_{\rm Gut}(t)/R_{\rm A}F_{\rm L}; \quad (16)$$

the expression $M_{{\rm P},\mathcal{T}}(t)$ (6), and $M_{\mathcal{T},{\rm P}}(t)$ (7); and the two external inputs $M_{\rm Gut}(t)$ and $M_{\rm Infuse}(t)$.

III. Equivalence of different peripheral tissue models

In this section we show that B and B' in Fig. 1(a) are identical. $M_{\rm Cap}(t)$ and $R_{\rm Cap}$ represent the characteristics of the capillary bed between the arterial side ($M_{\rm P}(t)$ and $R_{\rm P}$) and the venous side ($M_{\rm VC}(t)$ and $R_{\rm VC}$). Note that $R_{\rm VC} = R_{\rm Cap} = R_{\rm P}$ since there is no volume flow into the periphery. With B, $M_{\mathcal{T},{\rm P}}(t)$ is given in (7) which can also be written in the form $M_{\mathcal{T},{\rm P}}(t) = k_{\mathcal{T},{\rm P}}R_{\rm P}r\left(C_{\mathcal{T}}(t) - C_{\rm P}(t)\right)$. With B', $M_{\rm Cap}(t) = M_{\rm P}(t) - M_{{\rm P},\mathcal{T}}(t)$ which implies

$$\begin{aligned}C_{\rm Cap}(t) &= M_{\rm Cap}(t)/R_{\rm Cap}\\ &= C_{\rm P}(t) - k_{{\rm P},\mathcal{T}}r\left(C_{\rm P}(t) - C_{\mathcal{T}}(t)\right)\end{aligned} \quad (17)$$

since, by (6), $M_{{\rm P},\mathcal{T}}(t)$ can be written in the form $M_{{\rm P},\mathcal{T}}(t) = k_{{\rm P},\mathcal{T}}R_{\rm P}r\left(C_{\rm P}(t) - C_{\mathcal{T}}(t)\right)$. Furthermore, for B', $M_{\mathcal{T},{\rm P}}(t)$ is modified to $M_{\mathcal{T},{\rm P}}(t) = k_{\mathcal{T},{\rm P}}R_{\rm P}r\left(C_{\mathcal{T}}(t) - C_{\rm Cap}(t)\right)$. Therefore, $C_{\rm VC}(t) = M_{\rm VC}(t)/R_{\rm VC} = [M_{\rm P}(t) + M_{\mathcal{T},{\rm P}}(t) - M_{{\rm P},\mathcal{T}}(t)]/R_{\rm P}$ has one of two forms:

$$\begin{aligned}C_{\rm VC}(t) &= C_{\rm P}(t) - k_{{\rm P},\mathcal{T}}r\left(C_{\rm P}(t) - C_{\mathcal{T}}(t)\right)\\ &\quad + \begin{cases} k_{\mathcal{T},{\rm P}}r\left(C_{\mathcal{T}}(t) - C_{\rm P}(t)\right), & B\\ k_{\mathcal{T},{\rm P}}r\left(C_{\mathcal{T}}(t) - C_{\rm Cap}(t)\right), & B'\end{cases}\end{aligned} \quad (18)$$

B and B' are equivalent by the following argument. Insert (17) into the B' case of (18). First consider the case where $C_{\rm P}(t) \geq C_{\mathcal{T}}(t)$, simplify the $r(\cdot)$ functions in both cases of (18), and find that the two cases are identical. Second, consider the case where $C_{\rm P}(t) < C_{\mathcal{T}}(t)$, again simplify the $r(\cdot)$ functions in both cases of (18), and again find that the two cases are identical. Therefore B and B' are identical.

IV. Anomalous behavior of the standard model

The anomalous behavior of the 2-state model is the fact that the model can indicate that the mass flow of ethanol being degraded is greater than the mass flow of ethanol entering the liver. Since the liver in the 2-state model does not store ethanol, this is nonphysiological. The lower limit on the liver ethanol concentration can be computed as follows. The mass flux of ethanol entering the liver is

$$M_{\rm enter} = M_{\rm HA}(t) + M^{(2)}_{\rm PV}(t). \quad (19)$$

From (16), (15) and (19) the fundamental requirement is $M_{\rm Metab}(t) \leq M_{\rm enter}(t)$ which implies

$$M_{\max}/\left(R_{\rm HA} + R^{(2)}_{\rm PV}\right) - K_m \leq C_{\mathcal{L}}(t). \quad (20)$$

For a typical human subject, $M_{\max} = 300$mg/min, $R_{\rm HA} + R^{(2)}_{\rm PV} = 11.7$dL/min, and $K_m = 10$mg/dL so the lower limit on $C_{\mathcal{L}}(t)$ is 15.64mg/dL which is substantially below the level at which a human is intoxicated or at which data is recorded [9], [13]. For that reason, we have not been concerned with this characteristic of the 2-state model, although we have included a ramp function at the hepatic vein in order to guarantee that the mass flow of ethanol in the hepatic vein is nonnegative.

V. Numerical results

In the example the model is driven by an oral input which is a rectangular pulse of amplitude 2.4×10^4mg/min ethanol and duration 5 min. The resulting trajectories of the two- and three-state PBPK models are shown in Figure 1(b).The major feature of this simulation is the fact that the liver concentration exceeds the vascular concentration by nearly a factor of two and that the two- and three-state models predict substantially different peak concentrations. The reason that the liver concentrations are higher than the vascular concentrations (which are what is measured by a breath test) is that the ethanol from the gut travels via the portal vein directly to the liver where some of the ethanol is metabolized before entering the systemic vasculature. This is an important feature of ethanol kinetics because the liver toxicity of ethanol is related, at least in part, to the higher concentrations of ethanol present in the liver. Therefore, the three-state model is potentially more desirable than the two-state model because it allows a more accurate description of this important effect.

VI. Conclusion

The standard PBPK model and generalizations are described as systems of nonlinear differential equations.We show the equivalence of the different peripheral tissue models and the anomalous behavior of the standard PBPK model. The model demonstrates one of the causes of hepatic ethanol

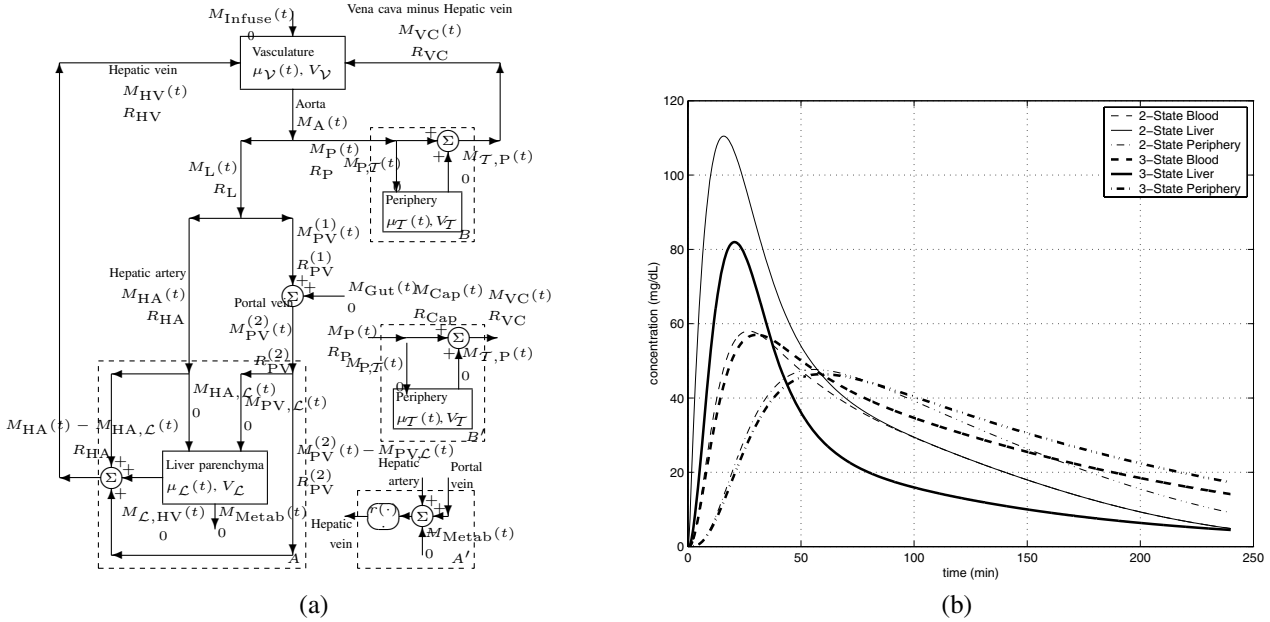

Fig. 1. Panel (a) shows Block diagrams for PBPK models. A complete three compartment model is shown. In addition, an alternative model for the liver (replace A by A') is shown which reduces the model to a two compartment model. In addition, an alternative model for the connection of the periphery (replace B by B') is shown. Panel (b) shows PBPK variable trajectories for the pulse oral input. The three (two) state variables for the three- (two-) state model are plotted.

toxicity which is the elevated ethanol concentration which the liver is subjected to due to the portal vein anatomy. Furthermore, models in differential equation form and with a limited number of parameters are key to system identification [14], filtering [15], and pattern classification [15] applications of these models to ethanol research studies in humans.

Modeling advances as described in this paper are central to determining mathematical models for individual subjects which will better predict the individual subjects' responses to ethanol. Using such models it will be possible to design dose trajectories for individuals such that all individuals have the same brain exposure to ethanol. If brain ethanol exposure can be controlled safely with no measurements, then novel experiments in imaging scanners can be performed that will provide new forms of information concerning ethanol.

REFERENCES

[1] M. A. Schuckit, T. L. Smith, G. P. Danko, J. Kramer, J. Godinez, K. K. Bucholz, J. I. Nurnberger Jr., and V. Hesselbrock, "Prospective evaluation of the four DSM-IV criteria for alcohol abuse in a large population," *American Journal of Psychiatry*, vol. 162, no. 2, pp. 350–360, Feb. 2005.

[2] H. D. Paykin, "A. alcohol dependence and abuse diagnoses: Concurrent validity in a nationally respresentative sample," *Alcoholism: Clinical and Experimental Research*, vol. 23, no. 1, pp. 144–150, Jan. 1999.

[3] D. Whitmire, L. Cornelius, and P. Whitmire, "Monte Carlo simulation of an ethanol pharmacokinetic model," *Alcohol Clin. Exp. Res.*, vol. 26, no. 10, pp. 1494–1493, 2002.

[4] T. K. Li, S. J. Yin, D. W. Crabb, S. O'Connor, and V. A. Ramchandani, "Genetic and environmental influences on alcohol metabolism in humans," *Alcohol Clin. Exp. Res.*, vol. 25, no. 1, pp. 136–144, 2001.

[5] S. L. Morzorati, V. A. Ramchandani, T. K. Li, and S. O'Connor, "A method to achieve and maintain steady state blood alcohol levels in rats using a physiologically-based pharmacokinetic model," *Alcohol*, vol. 28, pp. 189–195, 2002.

[6] M. H. Plawecki, R. A. DeCarlo, V. A. Ramchandani, and S. O'Connor, "Estimation of ethanol infusion profile to produce specified BrAC time course using physiologically based pharmacokinetic (PBPK) models based upon morphometrics," 2004, submitted.

[7] V. A. Ramchandani, T. K. Li, M. H. Plawecki, and S. O'Connor, "Mimicking the breath alcohol exposure following oral alcohol administration using IV ethanol infusions in healthy volunteers: Characterization of pharmacokinetic variability," 2004, submitted.

[8] P. Y. Kwo, V. A. Ramchandani, B. Sandhagen, L.-E. Bratteby, J. Gabrielsson, A. W. Jones, H. Fan, and R. G. Hahn, "Gender differences in alcohol metabolism: Relationship to liver volume and effect of adjusting for body mass," *Gastroenterology*, vol. 115, no. 6, pp. 1552–1557, 1998.

[9] V. A. Ramchandani, P. Y. Kwo, and T.-K. Li, "Influence of food and food composition on alcohol elimination rates in healthy men and women," *J. Clin. Pharmacol.*, vol. 41, pp. 1345–1350, 2001.

[10] Y. D. Neumark, Y. Friedlander, R. Durst, E. Leitersdorf, D. Jaffe, V. A. Ramchandani, S. O'Connor, L. G. Carr, and T.-K. Li, "Alcohol dehydrogenase polymorphisms influence alcohol-elimination rates in a male Jewish population," *Alcohol Clin. Exp. Res.*, vol. 28, pp. 10–14, 2004.

[11] M. G. Subramanian, S. H. Heil, M. L. Kruger, K. L. Collins, P. O. Buck, T. Zawacki, A. Abbey, S. K. J., and M. P. Diamond, "A three-stage alcohol clamp procedure in human subjects," *Alcohol Clin. Exp. Res.*, vol. 26, pp. 1479–1483, 2002.

[12] M. P. Boleda, P. Julia, A. Moreno, and X. Pares, "Role of extrahepatic alcohol dehydrogenase in rat ethanol metabolism," *Arch. Biochem. Biophys.*, vol. 274, pp. 74–81, 1989.

[13] R. P. Brown, M. D. Delp, S. L. Lindstedt, L. R. Rhomberg, and R. P. Beliles, "Physiological parameter values for physiologically based pharmacokinetic models," *Toxicol. Ind. Health*, vol. 13, pp. 407–484, 1997.

[14] M. H. Plawecki, "A physiologically-based pharmacokinetic (PBPK) model for ethanol: Mathematical foundations, parameter identification, and other applications," Ph.D. dissertation, Weldon School of Biomedical Engineering, Purdue University, West Lafayette, Indiana, USA, May 2005.

[15] J.-J. Han, "Stochastic models and nonlinear filtering algorithms for an ethanol biosensor," Ph.D. dissertation, School of Electrical and Computer Engineering, Purdue University, West Lafayette, Indiana, USA, 2006, tentative title and date.